Fuel 333 (2023) 126408

Contents lists available at ScienceDirect

Fuel

journal homepage: www.elsevier.com/locate/fuel

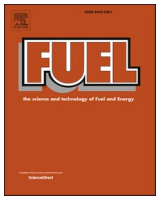

Full Length Article

GC–MS and ESI FT-ICR MS characterization on two type crude oils from the Dongying depression

Hanjing Zhang [a,b,*], Sumei Li [a,b,*]

[a] State Key Laboratory of Petroleum Resources and Prospecting, China University of Petroleum, Beijing 102249, China
[b] College of Geosciences, China University of Petroleum, Beijing 102249, China

ARTICLE INFO

Keywords:
ESI FT-ICR MS
Organic sulfur compounds
Maturity
Oil-oil correlation

ABSTRACT

Molecular-level characterization of sulfur-containing compounds has aroused much concern due to their relatively high abundance, sedimentary environment judgment and application at maturity. In this paper, saline lacustrine immature oils and freshwater lacustrine mature oils from the Dongying Depression (Bohai Bay Basin) were characterized by positive-ion electrospray ionization [(+) ESI] Fourier transform ion cyclotron resonance mass spectrometry (FT-ICR MS). The saline lacustrine oils are dominated by C_{20}-DBE_1, C_{30}-DBE_1, and C_{40}-DBE_3 which contain carbon skeletons of phytol, squalene and β-carotane respectively, denoting a genetic relationship between organosulfur compounds (OSCs) and their precursors. The precursors of C_{19}-C_{22} and C_{26}-C_{30} with DBE = 5 are derived from short-chain steranes and regular steroids, and their different contents can reflect the biological sources. The ratios of $C_{20}/(C_{19} + C_{21})$-DBE_1-S_1, $C_{40}/(C_{39} + C_{41})$-DBE_3-S_1, $C_{30}/C_{10\text{-}55}$-DBE_1-S_1 and $C_{27\text{-}29}/C_{10\text{-}55}$-$DBE_5$-$S_1$ are sensitive to organofacies, which are the first time used for oil-oil correlation. The novel maturity indices are based on the general process of thermally induced cyclization and aromatization of hundreds to thousands of OSCs from immature to mature oils. The high coefficient of correlations between the newly developed maturity parameters ($DBE_{6\text{-}16}/DBE_{1+2+5}$-$S_1$, $C_{35\text{-}60}/C_{10\text{-}35}$-$DBE_{1\text{-}17}$-$S_1$) with Ts/(Ts + Tm) and C_{29}-sterane αββ/(ααα + αββ) show that these utilities for assessing precisely the thermal maturity of lower maturity oils. The positive-ion ESI FT-ICR MS index has essential application prospects for organic input analysis, maturity evaluation, and oil-oil correlation.

1. Introduction

Sulfur is abundant in bitumens and crude oils; the total sulfur content varies from less than 0.05 % to 14 % by weight, but many crude oils contain less than 4 % sulfur [1,2]. Sulfur enrichment of organic matter may occur in the early diagenesis of sediments by quenching functional groups of hydrocarbons [3–5]. Sulfur is incorporated into the hydrocarbon functional groups intermolecularly to form macromolecular substances [6,7], and intramolecular sulfidation is another pathway to form OSCs [8]. The position of sulfur corresponds to the position of functional groups in precursor lipid molecules [9–13]. The result is that the information of precursor molecule will be preserved during diagenesis, which makes OSCs become the carrier of paleoenvironmental information. The formation of sulfur compounds will undergo geological changes such as burial or uplift, recording the thermal evolution history [14–18].

According to the different depositional environments, sulfur may react with the biopolymers and precursor molecules, or may enter the condensation crosslinking reaction to form sulfur-containing macromolecular compounds [19–21]. OSCs are inherited from kerogen and asphalt macromolecules and are usually more stable than their precursors [22–24]. There are many specific structures in the formation of OSCs, and their occurrence is primarily determined by environmental conditions [12,13,25–27]. Although thousands of OSCs with large molecular diversity are also reported in sediments, their indicative significance was not well investigated. Therefore, in this paper, the existence and formation of these compounds are applied as indicators for the geological environment. Biomarker maturity parameters can be reflected in different and restricted maturity ranges and can be used to estimate the maturity of crude oil relative to the oil window [28]. However, it is impossible to use classical biomarker ratios/parameters for special mature samples [28]. The non-biomarker maturity parameters cover a wider range of maturity [29]. Many scholars use NSO macromolecular compounds to establish maturity indicators [30,31],

* Corresponding authors at: State Key Laboratory of Petroleum Resources and Prospecting, China University of Petroleum, Beijing 102249, China.
E-mail addresses: 2281284825@qq.com (H. Zhang), smli@cup.edu.cn (S. Li).

https://doi.org/10.1016/j.fuel.2022.126408
Received 18 June 2022; Received in revised form 21 September 2022; Accepted 16 October 2022
Available online 28 October 2022

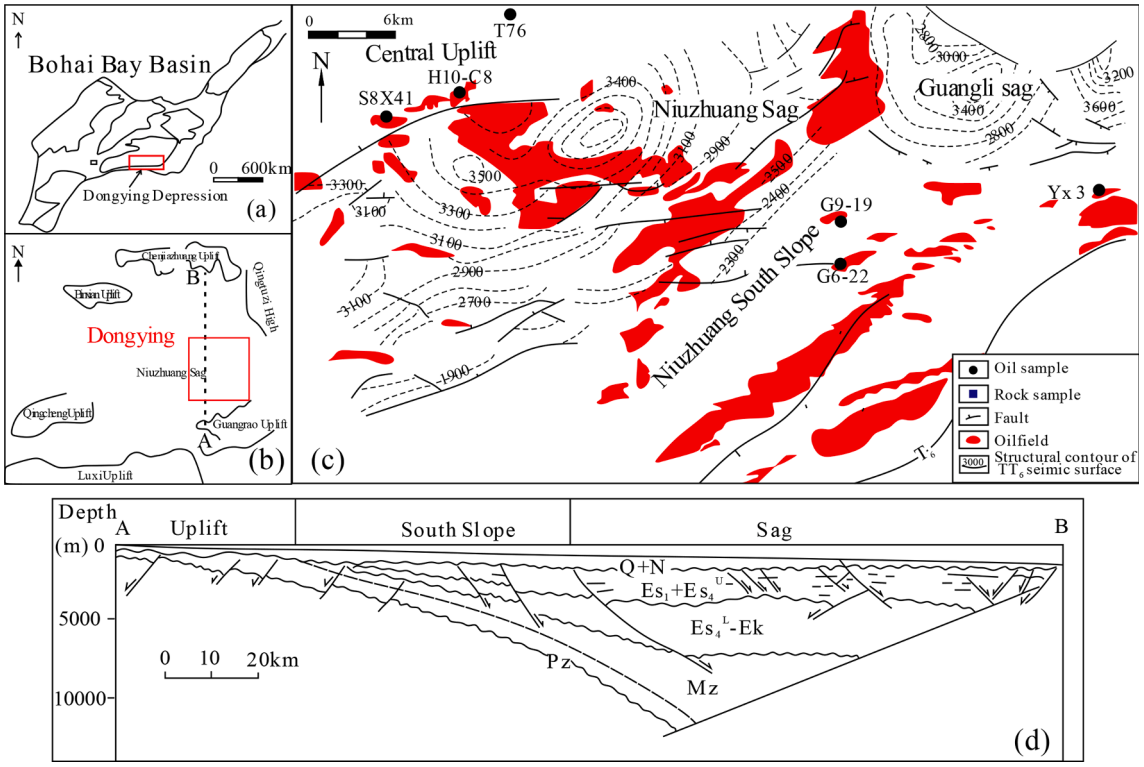

Fig. 1. Comprehensive geologic map of Dongying Depression. (a) Location of Bohai Bay Basin. (b) Dongying Depression. (c) Geological map of the study area. (d) Structural section and structural unit division in the Dongying Depression.

which have different discriminant parameters in different regions. However, these indicators are unsuitable for low mature oil in the study area. Unlike most commonly used maturity parameters, the novel parameters proposed are based on double bond equivalent (DBE) and carbon number.

Gas chromatography-mass spectrometry (GC–MS) is a common analytical and testing technology for organic sulfur compounds. For most geological samples, the content of organic sulfur compounds is often lower than that of other aromatic components (such as naphthalene and phenanthrene series), which will cover some organic sulfur compounds (OSCs) and lead to undetectable or rarely detectable OSCs by GC/MS [32]. Fourier-transform ion cyclotron resonance mass spectrometry (FT-ICR MS) combined with Electrospray ionization (ESI) should be used to obtain information from resin and asphaltine fractions regardless of whether the oil contains high or low sulfur compounds in aromatic fraction [33]. ESI FT-ICR MS is a recently developed powerful technique for characterizing organic sulfur compounds, especially those with high molecular weight in petroleum [34]. ESI FT-ICR MS has been used for petroleum geology applications based on its ultra-high resolving power and mass accuracy [35]. The combination of double bond equivalent (DBE) and molecular formula can be used to determine the specificity of some sulfur compounds in crude oil [36]. The construction and reliable application of maturity indices and oil-oil correlation are of great significance in petroleum exploration, but predicting maturity at a molecular level is still a major challenge. In this study, positive-ion ESI FT-ICR MS combined with GC–MS was used to investigate the composition and distribution of sulphur compounds in saline/freshwater lacustrine oils of different maturity in the Dongying Depression of the Bohai Bay Basin, and then the maturity and sedimentary environment influence on the OSCs were evaluated. Finally, The geochemical significance and genetic mechanism of OSCs were discussed.

2. Geological setting

The Bohai Bay Basin, located in the eastern part of China, is a Mesozoic Cenozoic fault basin developed on the North China Craton [37,38]. The Dongying Depression in the southeastern part of the Bohai Bay Basin is a typical lacustrine sub-basin containing abundant petroleum (Fig. 1a) [39]. Dongying Depression is bounded to the east by the Qingtuozi and Guangrao Uplift, to the west by the Qingcheng-Binxian Uplift, to the north by the Chenjiazhuang Uplift, and to the south by the Luxi Uplift (Fig. 1b). Dongying Depression is divided into Minfeng sag, Lijin sag, Niuzhuang sag and Boxing sag by several normal faults and central uplift belt [40,41]. Many asymmetric dustpan-like faulted depressions characterize Dongying Depression, and Paleogene is divided into Dongying Formation (Ed), Shahejie Formation (Es), and Kongdian Formation (Ed) from top to bottom (Fig. 1d) [42]. The Shahejie Formation can be further subdivided into Es_1 member, Es_2 member, Es_3 member, and Es_4 member. The tectonic evolution of the basin experienced the *syn*-rift stage and post-rift stage [43]. The lower Es_3 and upper Es_4 layers are produced during the expansion, rapid subsidence and contraction phases of the *syn*-rifting stage. The Shahejie (Es) Formation contains prominent reservoir-producing layers and two main sets of source rocks, including the Es_3 and Es_4 members [44–46]. The burital history of the area studied can be refered in Supplementary Fig. S1.

The targeted oil in the study area is mainly Niuzhuang sag and the central uplift belt in Dongying Depression (Fig. 1c), which came from two distinct sedimentary facies: saline lacustrine in the Es_4 member and freshwater lacustrine in the Es_3 member [44,45].

3. Samples and methods

Two different types of oils were studied (Table 1): the first type of crude oil was collected from Es_4 member of Shahejie Formation in the South Slope of the Niuzhuang Sag (SSNS) of the Dongying Depression; the second type of crude oil was collected from Es_3 member of Shahejie

Table 1
Basic characteristics of crude oil from the Dongying Depression.

Location	Well	Strata	Depth (m)	Pr/Ph	CPI	OEP	Pr/nC_{17}	Ph/nC_{18}	nC_{21}/nC_{22}^{+}	C_{29} 20S	$C_{29}\alpha\beta\beta$	$C_{31}H$	Ts	G/$C_{30}H$	$C_{35}/C_{34}H$	Tri/H	DBT/P	Rc1	Rc2
CU	*H*10-C8	Es_2	2321.1–2350.9	1.05	1.08	1.11	0.57	0.65	0.86	0.51	0.43	0.58	0.54	0.07	0.60	0.075	0.10	0.69	0.63
	S8X41	Es_1	2453.4–2455.6	1.06	1.09	1.09	0.59	0.67	0.73	0.52	0.45	0.58	0.57	0.08	0.58	0.079	0.09	0.70	0.65
	T76	Es_4	3340.5–3461	1.49	1.20	1.13	1.04	0.86	1.04	0.45	0.37	0.59	0.36	0.08	0.63	0.090	0.12	0.67	0.60
SSNS	G6-22	Es_3	1678–1674.8	0.38	0.98	0.92	1.22	3.48	1.57	0.34	0.30	0.57	0.34	0.92	0.97	0.108	0.52	0.72	0.59
	Yx3	Es_4	1810–1904	0.45	0.96	0.93	1.88	6.70	1.56	0.21	0.24	0.55	0.25	0.75	0.66	0.169	0.39	0.80	0.80
	G9-19	Es_4	2380	0.38	0.96	0.95	1.20	2.79	0.89	0.36	0.32	0.55	0.33	0.90	1.22	0.117	0.36	0.73	0.69

Note: CU: the Central Uplift; SSNS: South slope of the Niuzhuang sag; Pr/Ph: pristane/phytane; CPI: $[(C_{25}+C_{27}+C_{29}+C_{31}+C_{33})/(C_{26}+C_{28}+C_{30}+C_{32}+C_{34})+(C_{25}+C_{27}+C_{29}+C_{31}+C_{33})/(C_{24}+C_{26}+C_{28}+C_{30}+C_{32})]/2$; OEP: $(C_i+6\,C_{i+2}+C_{i+4})/(4\,C_{i+1}+4\,C_{i+3})$ or $(4\,C_{i+1}+4\,C_{i+3})/(C_i+6\,C_{i+2}+C_{i+4})$, among which i + 2 is the maximum peak of *n*-alkanes with i corresponding I to odd and even member respectively (Scalan and Smith, 1970);; Pr/nC_{17}: pristane/nC_{17}; Ph/nC_{18}: phytane/nC_{18}; nC_{21}/nC_{22}^{+}: $\sum nC_{21}/\sum C_{22}^{+}$; C_{29}20S: C_{29}-sterane ααα20S/(20S + 20R); $C_{29}\alpha\beta\beta$: C_{29} sterane αββ/(ααα + αββ); $C_{31}H$: C_{31} hopanes 22S/(22S + 22R); Ts: Ts/(Ts + Tm); G/$C_{30}H$: Gammacerane/C_{30}-Hopane; $C_{35}/C_{34}H$: C_{35}-hopane/C_{34}-hopane; Tri/H: Tricyclic terpane /Hopanes; DBT/P: Dibenzothiophene/Phenanthrene; Rc1 = 0.55*MPI1 + 0.44 [55]; Rc2 = −0.166 + 2.242 × F1, F1 = [(2-MP)+(3-MP)]/[(2-MP)+(3-MP)+(1-MP)+(9-MP)] [56].

Formation in the Central Uplift (CU) of Dongying Depression. The SSNS oils are featured by high density (0.9385 g/cm^3–0.9553 g/cm^3), high viscosity (653.33 mPa.s–1500.46 mPa.s), low freezing point (−10 °C to 9.7 °C), and relatively high sulfur content (1.60 %–1.85 %), which are also common characteristics of low-mature oil. The CU oils were featured by relatively low density (0.8523 g/cm^3–0.8976 g/cm^3), low viscosity (7.95 mPa.s–86.3 mPa.s, high freezing point (28 °C–35 °C), and low sulfur contents (0.25 %–0.56 %), which were significantly different from the SSNS oils. FT-ICR MS and GC–MS analyzed the samples, and the results are shown in Tables 1 and 2.

3.1. GC–MS

After asphaltene precipitation, saturated hydrocarbons were fractionated from crude oil on neutral alumina by *n*-hexane elution, and then aromatic hydrocarbons were separated by *n*-hexane and dichloromethane mixed solution (volume ratio 1: 2) elution. GC–MS analyses were performed using a Hewlett-Packard 5890 GC coupled to a Mass Selective Detector fitted with an HP-1 fused silica column (30 m × 0.25 mm i.d. × 0.25 μm film thickness). For analyzing saturate fractions, the GC column was held at 50 °C for 2 min, ramped to 100 °C at a rate of 2 °C/min and then to 310 °C at 3 °C/min, with a final temperature holding time of 15 min. For analyzing aromatic hydrocarbons, the GC column was held at 60 °C for 2 min, ramped to 150 °C at a rate of 8 °C/min, and then to 320 °C at 4 °C/min, with a final temperature holding time of 10 min. Helium as a carrier gas has the electron-impact ionization (EI) energy of 70 eV [27].

3.2. FT-ICR MS analysis

Fourier transform ion cyclotron resonance mass spectrometry (FT-ICR MS) analysis, the first sulfur compound methylation experiment sample preparation [47]. The crude oils 100 mg, three times methyl derivatization reaction, each diluted with 2 mL dichloroethane sample, adding 50 μL iodomethane, 2 mL 0.5 mol/L silver tetrafluoroborate dichloroethane solution, ultrasonic shock mixing uniform, dark conditions, standing for 24 h. Centrifuging the solution after the reaction, removing the silver iodide precipitate, and extracting the remaining materials with *n*-hexane to obtain a thiophenium salt solution.

The prepared samples were used for FT-ICR MS analysis. The instrument was Apex-Ultra 9.4 T type from Bruker, USA. The sample solution was infused with positive-ion electrospray ionization (ESI) source at 250 μL /h, −4 kV emitter voltage, −4.5 kV capillary column introduced voltage, and 320 V capillary column end voltage by using a syringe pump. A hexapole DC voltage of ion is 2.4 V, RF 300 Vp-p; ions accumulated time is 0.1 s. The optimized mass of Q1 was 250 Da. The operating conditions of the quadrupole collision pool are 5 MHz, 400 Vp-p, and the ion accumulated time is 1 s. The transition time for electrostatic focusing to convert ions into ICR was set to 1.1 ms. The working conditions of ICR mass spectrometry are excitation attenuation 11.75 db, mass range 200–750 Da, data size 4 M, and time-domain signal superposition 64 times. The data processing method is shown in the literature [33,34].

3.3. Pearson's correlation

The Pearson correlation coefficient [48] is also called Pearson product-moment correlation coefficient (PPMCC). It describes the close degree of connection between two fixed distance variables and is used to measure the correlation (linear correlation) between two variables X and Y. Its value is between −1 and 1. It is generally expressed by r, and the calculation formula is.

$$r_{xy} = \frac{n\Sigma XY - \Sigma X\Sigma Y}{\sqrt{\left[N\Sigma X^2 - (\Sigma X)^2\right]\left[N\Sigma Y^2 - (\Sigma Y)^2\right]}}$$

Table 2
Parameters calculated by the results of positive-ion ESI FT-ICR MS for the oils and source rocks.

well	Content/%					A	B	C	D	E	F
	N_1S_1	O_1S_1	O_1S_2	S_1	S_2						
*H*10-C8	0	0	0	100.0	0	0.569	0.549	0.129	0.060	1.826	1.343
S8X41	28.4	7.4	0	60.6	3.6	0.679	0.671	0.114	0.055	4.204	1.793
T76	0.0	39.9	0	52.2	7.9	0.569	0.756	0.184	0.057	2.930	0.836
G6-22	0.6	1.8	0	94.8	2.7	0.813	2.002	0.404	0.071	0.225	0.286
YX3	0.8	4.5	0	94.7	0.0	0.899	2.309	0.402	0.099	0.332	0.277
G9-19	0.9	2.3	2.1	90.4	4.3	0.784	1.628	0.366	0.067	0.293	0.377

Note: A: $C_{20}/(C_{19}+C_{21})$-DBE_1-S_1 (The ratio of C_{20} homologs to C_{19} and C_{21} homologs of the S_1 species with DBE = 1); B: $C_{40}/(C_{39}+C_{41})$-DBE_3-S_1(The ratio of C_{40} homologs to C_{39} and C_{41} homologs of the S_1 species with DBE = 3); C: C_{27-29}/C_{10-55}-DBE_5-S_1 (The ratio of C_{27-29} homologs to C_{10-55} homologs of the S_1 species with DBE = 5); D: C_{30}/C_{10-55}-DBE_1-S_1(The ratio of C_{30} homologs to C_{10-55} homologs of the S_1 species with DBE = 1); E: DBE_{6-16}/DBE_{1+2+5} -S_1 (The ratio of sum of DBE = 6–16 to that of the DBE = 1, 2, 5 of the S_1 species); F: C_{35}^{+}/C_{34}^{-}-DBE_{1-17}-S_1 (The ratio of C ≥ 35 homologs to C ≤ 34 homologs of the S_1 species with DBE = 1–17).

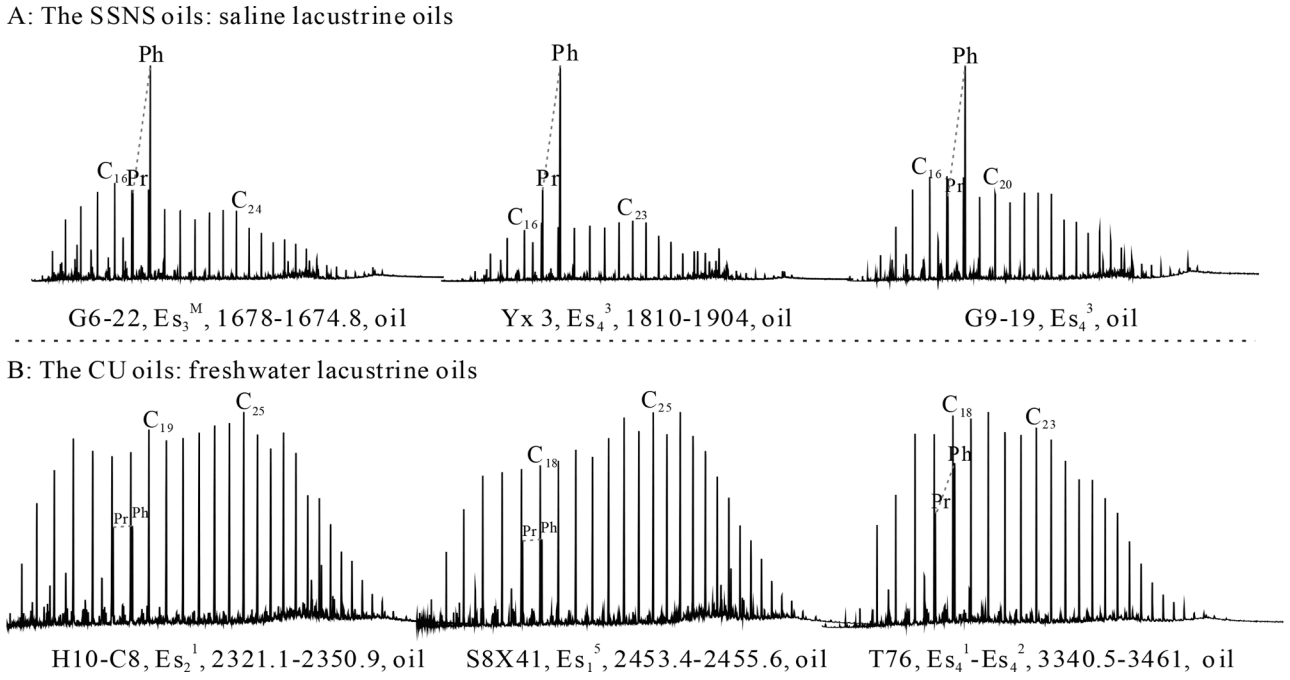

Fig. 2. Total ion chromatograms (TIC) of saturate from crude oils.

n is the sample size; X and Y are the observed values of two variables.

If r > 0, the two variables are positively correlated; if r < 0, the two variables are negatively correlated. 0.8 < |r| ≤ 1.0 is highly correlated; 0.6 < |r| ≤ 0.8 is strong correlation; 0.4 < |r| ≤ 0.6 is moderate correlation; 0.2 < |r| ≤ 0.4 is weak correlation; 0.0 ≤ |r| ≤ 0.2 is extremely weakly correlated or irrelevant.

4. Geochemical characteristics and classification of the crude oils

4.1. Molecular compositions and oil families of the crude oils

4.1.1. Hydrocarbon biomarkers

Total ion chromatograms (TICs) from the saturate fractions of the oils are shown in Fig. 2. Most oils had a bimodal distribution of *n*-alkanes (nC_{12}–nC_{37}), suggesting both microbial and higher plant contributions [49]. The long-chain *n*-alkanes likely have a higher plant origin, although they can derive from other sources (e.g., *Botryococcus braunii*) [50]. Oils located on the South slope of the Niuzhuang Sag (SSNS) in the Dongying Depression have relatively low Pr/Ph values (0.2–0.3), consistent with deposition in a hypersaline environment [28]; while the Central Uplift (CU) freshwater lacustrine oils have higher Pr/Ph values (0.9–1.3), indicating a weakly oxidizing to weakly reducing environment [51]. The carbon preference index (CPI) and odd–even predominance (OEP) values are 0.96–1.20 and 0.92–1.13, respectively, showing no obvious trends. The nC_{21}^{-}/nC_{22}^{+} ratios of the SSNS oils and the CU oils are 0.89–1.57 (average 1.34) and 0.73–1.04 (average 0.88) (Table 1), respectively, which could be affected by kerogen type, thermal maturity and second alteration.

The saline lacustrine oils in the South slope of the Niuzhuang Sag have a significantly high amount of gammacerane (Fig. 3). The ratios of gammacerane/C_{30} hopane were 0.75–0.92 (average 0.86) (Table 1). The generally high content of gammacerane in oils indicates saline conditions or a stratified water column during source rock deposition [52]. Another distinguishing characteristic of the SSNS oils is an obvious predominance of C_{35} and C_{34} hopanes (C_{35}/C_{34} = 0.66–1.22, average 0.95) (Table 1), which coincides with the features of typical saline lacustrine oils. The CU oils exhibited lower ratios of gammacerane/C_{30} hopane (0.07–0.08) (Table 1) and C_{35}/C_{34} hopane 0.58–0.63, average 0.60) (Table 1), suggesting that the source rocks were deposited in a freshwater environment. No or little biodegradation of the crude oil was interpreted from the TIC and *m/z* 177 mass chromatograms of the oil-saturated fractions because there was no obvious depletion of *n*-alkanes or presence of C_{25} norhopanes.

The fingerprints of the C_{27}, C_{28} and C_{29} regular steranes in the SSNS and CU oils showed either a "V" shape due to relatively low C_{28} steranes

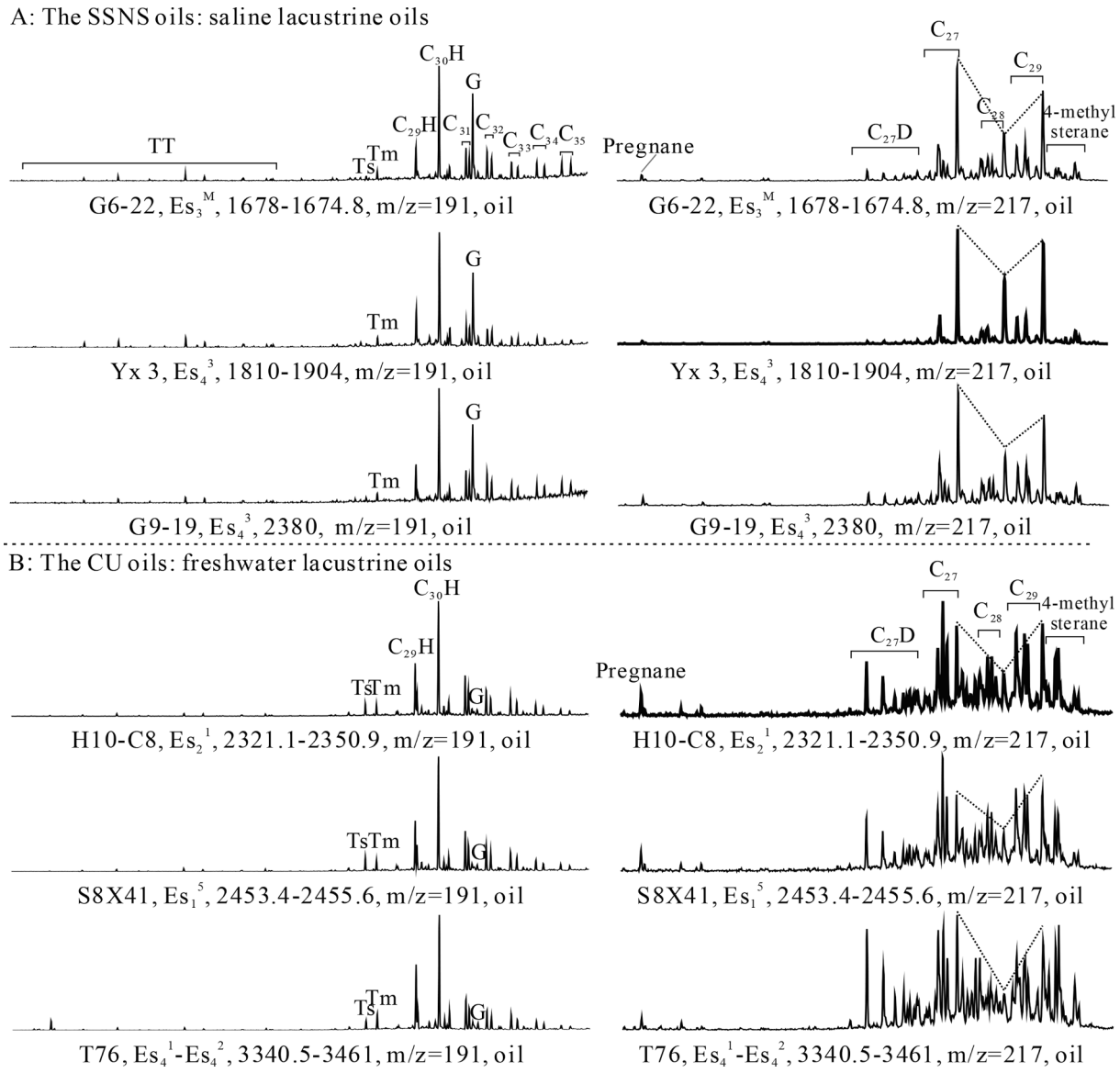

Fig. 3. Mass chromatograms of *m/z* 217and *m/z* 191 of saturates for crude oils.

(Fig. 3). C_{27} steroids are indicative of algal input, while C_{29} steroids may come from both algae and higher plants [53]. A relative predominance of C_{27} ααα (20R) to C_{29} ααα (20R) for the crude oils, i.e., G6-22, YX3 and G9-19, with a relatively low thermal maturity may reflect a higher contribution of algae to the oil precursors (Fig. 3). The ratios of C_{29}-sterane ααα20S/(20S + 20R) and C_{29}-sterane αββ/(ααα + αββ) of the SSNS oils are 0.24–0.38 and 0.24–0.32, respectively (Table 1), demonstrating the these were low-mature oils (Fig. 4c). The C_{29}-sterane ααα20S/(20S + 20R) and αββ/(ααα + αββ) values of the CU oils ranged from 0.42 to 0.61 and from 0.37 to 0.45, respectively, reflecting these mature oils (Fig. 4c). However, the "low maturity" from the C_{29}-steranes could be attributed to that sulfurization is more easily on C_{29}-αββ and the transformation from C_{29}-20R to 20S, because the diagenetic pathway of such Δ^7 sterols in hypersaline environments, might rapidly lead to the formation of 20R and 20S 5α(H), l4β(H), l7β(H)- steranes [54]. Nevertheless, the Ts/(Ts + Tm) ratios for the SSNS and CU oils are in the ranges of 0.25–0.34 and 0.36–0.57, respectively, suggesting relatively low maturity of the former.

Aromatic hydrocarbons in the SSNS and CU oils are mainly composed of naphthalene, phenanthrene, dibenzothiophene and triaromatic steranes (Fig. 4). Aromatics have polycyclic structure and high thermal stability, which are often used to determine the thermal maturity of samples. Equivalent vitrinite reflectance calculated from MPI1 (Rc1 = 0.55MPI1 + 0.44, suitable for Ro = 0.65 %−0.35 %; Rc1 = -0.50 × MPI1 + 2.27, suitable for Ro = 1.35 %−2.00 %) and Equivalent vitrinite reflectance calculated from F1 (Rc2 = -0.166 + 2.242 × F1, F1 = [(2-MP)+(3-MP)]/[(2-MP)+(3-MP)+(1-MP)+(9-MP)]) [55,56] was used to evaluate the maturity of the crude oils analyzed, respectively. The Rc1 and Rc2 of the CU oils are in the ranges of 0.67 %–0.70 % and 0.60–0.65, respectively, which are consistent with the biomarker maturity parameters. However, the equivalent vitrinite reflectances values (Rc1 and Rc2) for the SSNS oils are unnormally larger than that of the CU oils, which are not consistant with biomarker indices and might be something misleading (Table 1). Methylphenanthrene index migh be unsuitable to calcurate equivalent vitrinite reflectance for the brackish-saline oil with relatively low maturity.

4.1.2. *Genetic types of crude oils*

Two distinct groups of oils were identified based on biomarker parameters and related cross plots (Fig. 5a–d). The SSNS oils (G6-22, YX3, G9-19) and CU oils (H10-C8, S8X41, T76) are derived mixtures from type I and II kerogen by the pristane/*n*-C_{17} versus phytane/*n*-C_{18} plot

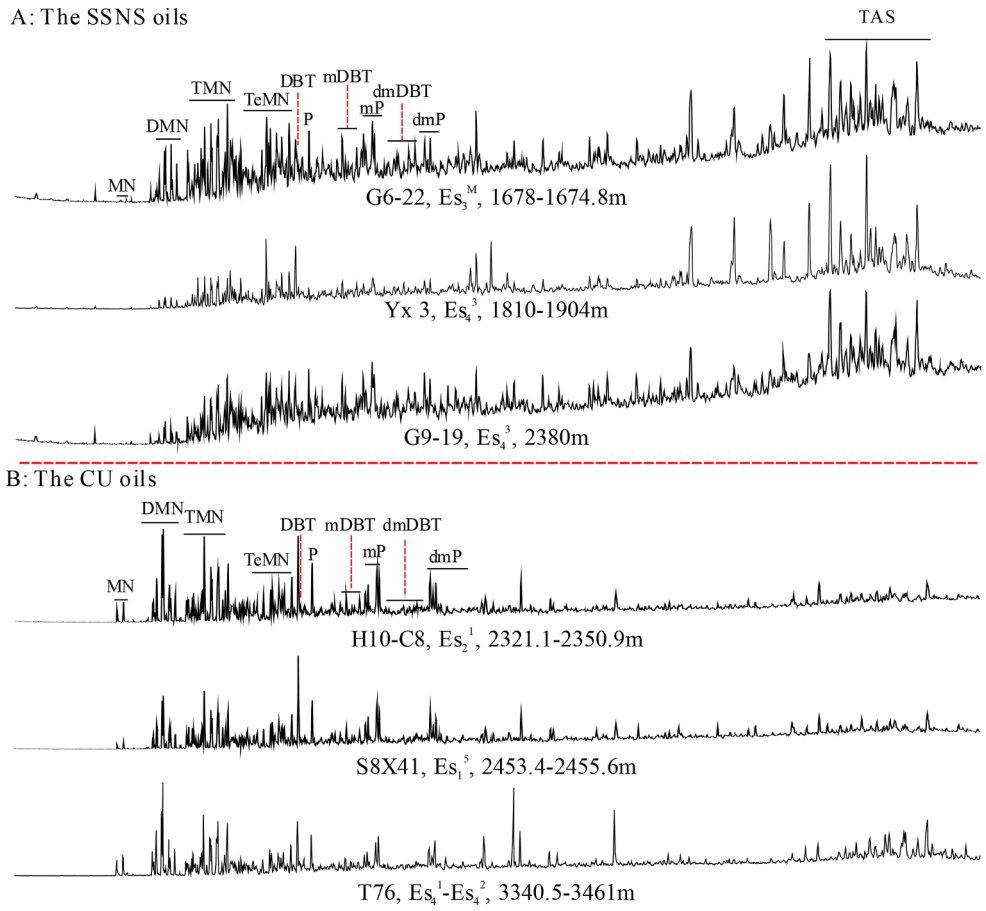

Fig. 4. Total ion chromatogram of the aromatic from the oils in the Dongying Depression (MN: methyl-; DMN: dimethyl-; TMN: trimethyl-; TEMN: tetramethyl-naphthalene; DBT: dibenzothiophene; MDBT: methyl-; DMDBT: dimethyl-; TMDBT: trimethyl-dibenzothiophene; P: Phenanthrene; mP: Methyl-phenanthrenes; dmP: dimethyl-phenanthrene; TAS: triaromatic steranes).

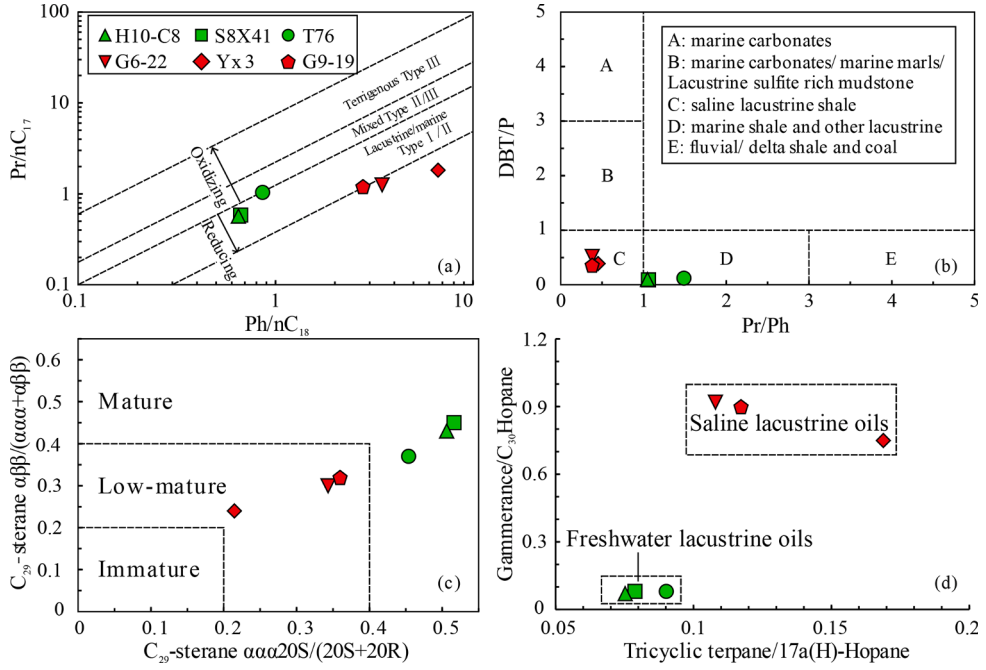

Fig. 5. Cross plots of biomarkers showing two oil families for the investigated oils from the Dongying Depression [51,57].

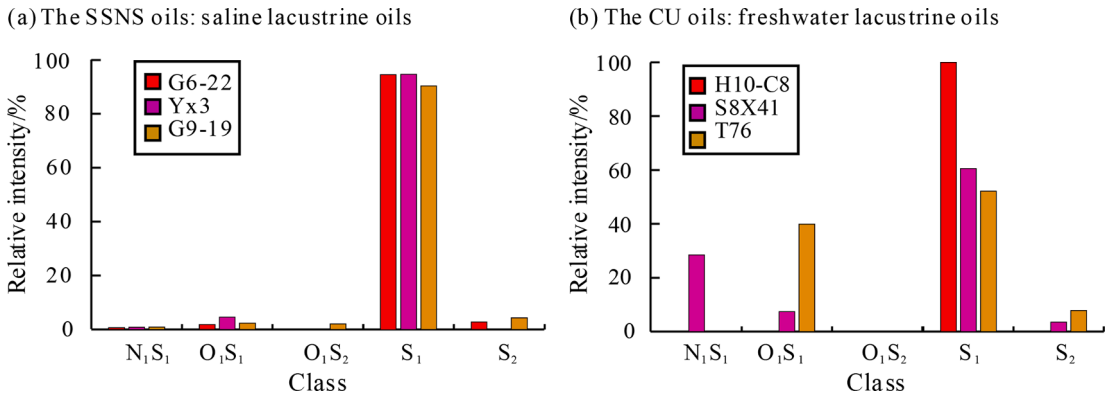

Fig. 6. Relative abundance of heteroatom class species in the oils assigned from positive-ion ESI FT-ICR MS.

(Fig. 5a, Table 1). The cross plot of pristane/phytane (Pr/Ph) against dibenzothiophene/phenanthrene (DBT/P) (Fig. 5b) was used as a paleoenvironment proxy [9]. The SSNS oils aggregated in section C, represent a saline lacustrine environment whereas the CU oils grouped in section D indicate freshwater lacustrine facies (Fig. 5b). The parameters C_{29}-sterane ααα20S/(20S + 20R) and C_{29} sterane αββ/(ααα + αββ) are the most commonly used indicators for less mature and mature oils. This parameter shows that SSNS oils are low mature oil, CU oils are mature oil (Fig. 5c). The ratios of gammacerane/C_{30} hopane, and Tricyclic/pentacyclic terpanes all divide the oils into two families (Fig. 5d).

The SSNS and the CU oils are due to two different oil families with different source rocks (Fig. 2–5). The previous oil-source rock correlation showed that the SSNS oils were mainly derived from the Es_4 source rocks deposited in typical brackish-saline lacustrine facies, while the CU oils were derived from typical freshwater lacustrine facies [40,44].

4.2. Positive-ion ESI FT-ICR MS oil characterization

4.2.1. Composition and distribution of sulfur-containing compounds

Five sulfur-containing compounds, including S_1 (molecules with one sulfur atom), O_1S_1, O_2S_1, S_2 and N_1S_1 (Fig. 6), were detected in the crude oils from the Dongying Depression by positive-ion ESI FT-ICR MS. The dominant (in relative mass peak abundance) class species in the SSNS oils is S_1 (90.4–94.8 %, average 93.3 %), with quite a little or trace amount of the species of O_1S_1 (1.8–4.5 %, average2.9 %), N_1S_1 (0.6–0.9 %, average 0.8), S_2 (0–4.3 %, average 2.3 %), O_1S_2 (0–2.1 %, average 0.7 %), and $N_1O_1S_1$ (Fig. 6a; Table 2). S_1 species also predominate in the CU oils, ranging in 52.6–100 % (average 70.9 %), having a little higher concentration of N_1S_1 (average 9.5 %), O_1S_1 (average 15.8 %) and S_2 (average 3.8 %) than those of the SSNS oils (Table 2; Fig. 6).

4.2.2. Composition and distribution of S_1 class species

The composition of S_1 class species in the crude oils analyzed by positive-ion ESI FT-ICR MS is shown in Fig. 7. The double bond equivalent (DBE) values and carbon numbers of the S_1 class species ranged from 1 to 15 and from 10 to 54, respectively, in SSNS. CU oils have a wider range of DBEs and carbon numbers, 1–17 and 10–57, respectively.

The S_1 species with DBEs of 0, 1, 2 and 3 are most likely to be cateniform thioether series compounds, one cyclic thioethers, two cyclic thioethers, and cyclic thioethers with three rings or thiophene series, respectively. Higher DBE values mean more possible structures for identified OSCs [29,33]. Some of the other compounds were benzo homologues of two cyclic-ring OSCs. As shown in Fig. 7, the lower abundance of S_1 species with DBE = 0 indicates no or deficient concentrations of alkyl OSCs in the SSNS oils and CU oils. The content of DBEs is related to maturity. From SSNS oils (low mature oils) to CU oils (mature oils), the main peak of DBE shifted from DBE = 1 to DBE = 6 (Fig. 7a–f), that is, the value of DBEs increased with the increase of maturity. Relatively high concentration of the S_1 species with DBE ≤ 8 presented in the SSNS oils, indicating that the content of compounds with low stability is higher and the maturity is lower; S_1 species with relatively high DBEs were detected in CU oils (Fig. 7a–f), reflecting probably a relatively high thermal maturity.

Sulfur compounds are typical heteroatoms in crude oil. They are usually formed by the combination of inorganic sulfides (S, HS^-, HS_x^-, and S_x^{2-}) with hydrocarbons and carbohydrates containing active functional groups (such as carbon–carbon double bonds) during early diagenesis [58,59]. Organic sulfur compounds are structurally similar to these hydrocarbons and carbohydrates. OSCs with a special structure related to the sedimentary environment. For instance, the abundance of C_{20} with DBE = 1 in SSNS oils is very high (Fig. 7g–i, m–o), which was possibly derived from phytol via intramolecular sulfurization and hydrogenation [26,33]. Therefore, the carbon skeleton of C_{20} with DBE = 1 in the SSNS oils is similar to that of phytanic acid and phytol, which is consistent with high abundant phytane judged by GC–MS analysis. Similarly, the high abundance of C_{40} with DBE = 3 (Fig. 7g–i, m–o) could be derived from the β-carotane via intramolecular sulfurization and hydrogenation during early diagenesis [32]. Terpenoid sulfides are commonly found in low-mature oil, and isoprenoids containing C_{20} and C_{40} are predominant (The possible structure of the compound is shown in Fig. 7h, g). The detected C_{30} sulfide is a single ring terpenoid sulfide of the squalane skeleton. The bio-precursor of C_{30}-DBE_1 sulfide detected in this study is squalene [4,12]. In addition, a higher percentage of C_{19}-C_{22} and C_{26}-C_{30} in SSNS and CU oils (Fig. 7) is precisely consistent with the carbon numbers of short-chain steranes and regular steroids by GC–MS analysis. Due to the widespread sulfurization of steroids in many compounds in sediments, only steroids have more double bonds, hydroxyl groups and carbonyl groups [60]. These groups are easy to combine with inorganic sulfur, resulting in natural vulcanization. Therefore, C_{19}-C_{22} and C_{26}-C_{30} have similar carbon skeletons to steroids and the possible structure of the compound is shown in Fig. 7i.

5. Controls and implications of sulfur-containing compounds

5.1. Sedimentary environment and oil-oil correlation

With the development of FT-ICR MS, the understanding of organic sulfur compounds has become more comprehensive, and many OSCs with structural units have been identified. Sulfur-containing structural units in geological macromolecules are generally related to the sedimentary environment, showing distinct biological inheritance signs. Therefore, these OSCs have great potential as molecular indicators for the sedimentary environment and oil-oil correlation.

OSCs with a wide range of DBEs and carbon numbers in crude oil are generally produced by their corresponding non-sulfur compounds (heteroatomic compounds without sulfur). In SSNS oils, a relatively high peak of OSCs is C_{20} compounds with DBE = 1 (Fig. 7m–o) abundance of $C_{20}H_{43}S_1$ (Structure in Fig. 7f), which is similar to the carbon skeleton of

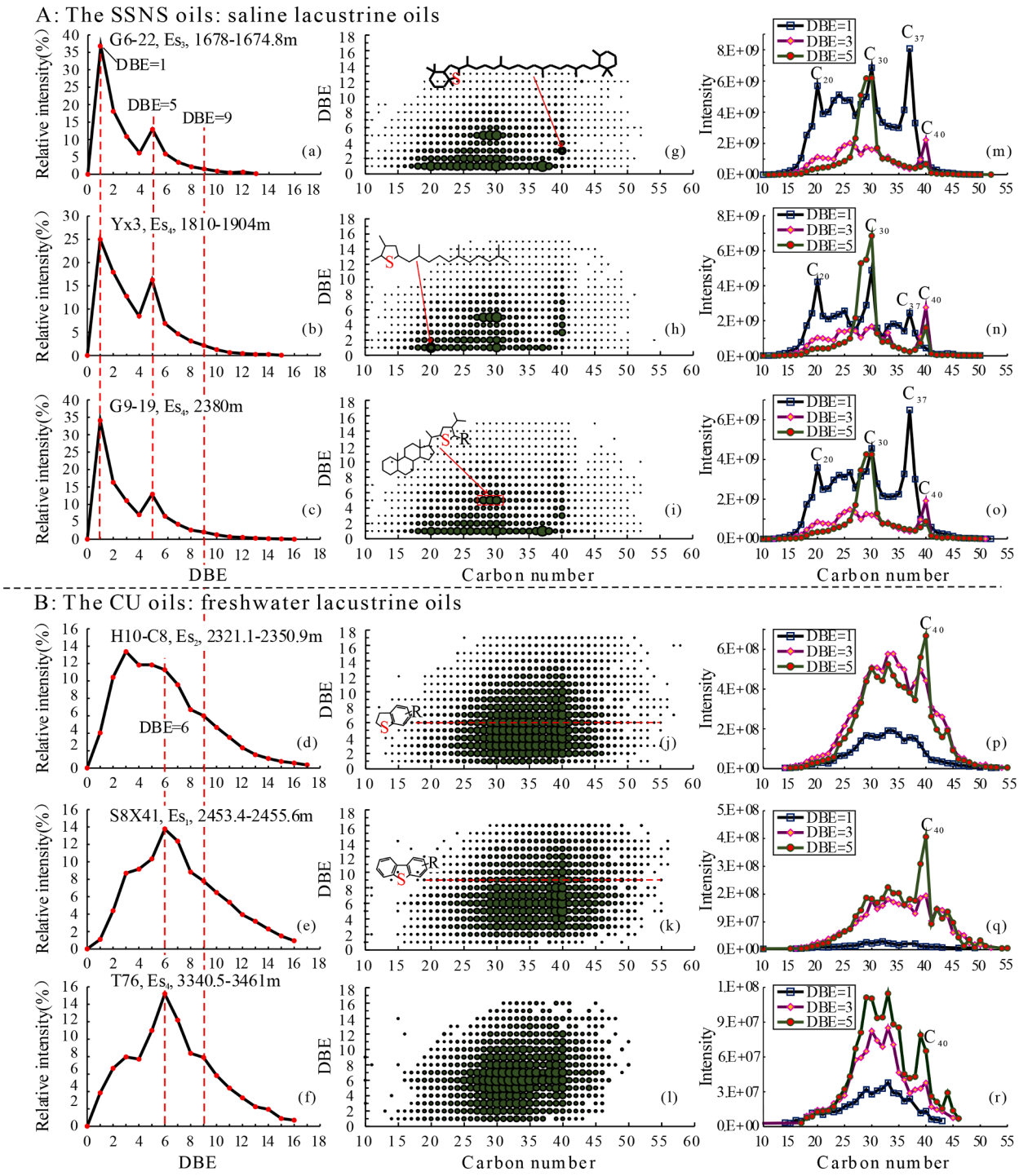

Fig. 7. Relative intensity/abundance of S_1 class species with various DBE values for the crude oil detected by positive-ion ESI FT-ICR MS; Plots of DBE versus carbon number of S_1 class species for the selected oils; Carbon curve of the S_1 class species with DBE = 1, 3 5 for the selected oils.

phytol and reflects the reduction environment. Compared with CU oils, the peak of C_{30}-DBE_1 sulfide with a bio-precursor of squalene is also higher in SSNS oils (Fig. 7), reflecting a strictly anaerobic condition. The abundance of C_{40} compounds with different DBEs is very high in SSNS oils. These compounds are similar to the β-carotane skeleton structure of the cyclic sulfide compounds, reflecting pigment source or salt-lake facies deposition. The carbon number is C_{28}-C_{30} compounds with DBE = 5 sulfur compounds, which are thioether steranes, reflecting organic input.

Therefore, organic sulfur compounds with special structures can be used for oil-oil correlation. As shown in Fig. 8, these parameters (e.g., $C_{20}/(C_{19}+C_{21})$-DBE_1-S_1, $C_{40}/(C_{39}+C_{41})$-DBE_3-S_1, C_{30}/C_{10-55}-DBE_1-S_1, C_{27-29}/C_{10-55}-DBE_5-S_1) can be used for oil-oil correlation, and the comparison results are the same as those of GC–MS analysis. Although there are few samples, significant differences in the structure of some organic sulfur compounds between freshwater and saline crude oil samples can also be observed (Figs. 7 and 9). It shows that ESI-FT-ICR MS analysis has the potential to distinguish different types of lacustrine samples.

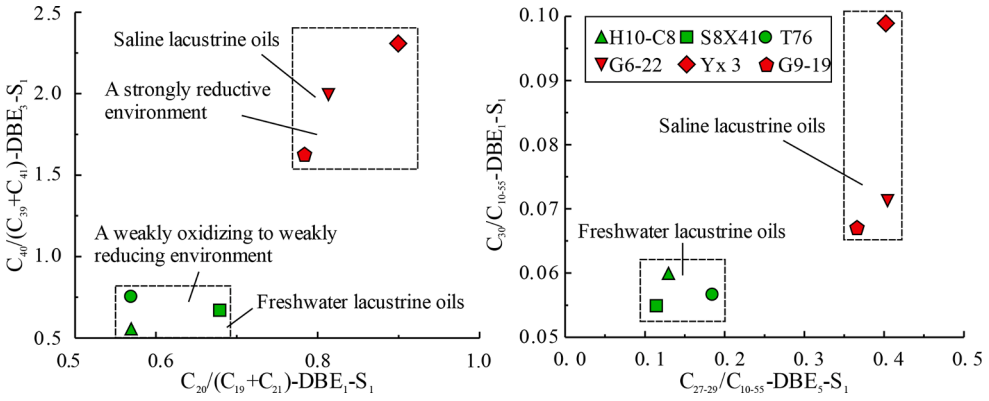

Fig. 8. Oil-oil correlation of S_1 class species of OSCs parameters by (+) ESI FT-ICR MS.

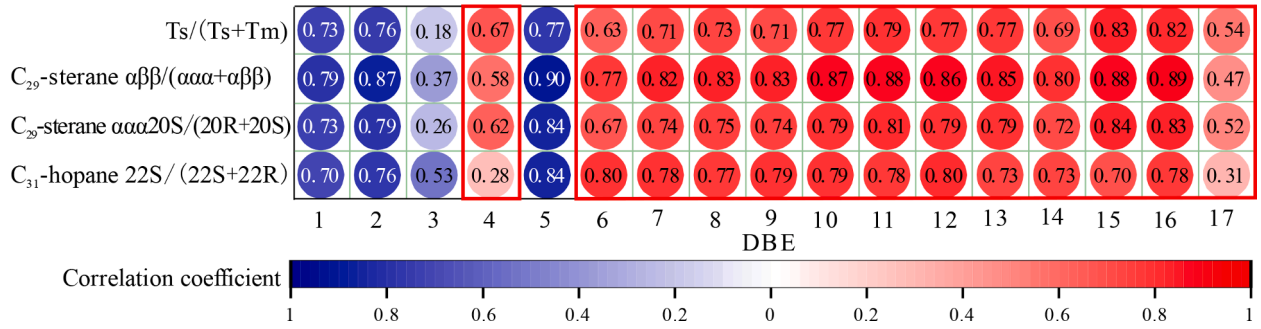

Fig. 9. DBE percentage-to-maturity parameters of GC–MS comparisons using Pearson's correlation are represented numerically by $|r|$-values and in shades of red (positive correlation) and blue (negative correlation) in SSNS and CU oil. (DBE percentage" means the percentage of the sum of the S_1 species with a specific DBE value (i.e., DBE_1-S_1) among the total S_1 species (with DBE = 1 ~ 17). For example, the X-axis is 1, and the Y-axis is C_{31} 22S/(22S + 22R), which represents the negative correlation and the correlation coefficient $|r| = 0.70$ between abundance of DBE = 1 and the maturity parameter of C_{31} 22S/(22S + 22R). The meanings of other lattices in the figure are similar. The number represents the correlation coefficient r, and the color represents the positive or negative correlation.). (For interpretation of the references to color in this figure legend, the reader is referred to the web version of this article.)

5.2. Novel maturity indices

After forming organic OSCs, they will undergo a series of physical and chemical changes, providing geochemical maturity indicators. The C_{29}-sterane ααα20S/(20S + 20R) and C_{29}-sterane αββ/(ααα + αββ) values of six crude oil samples were 0.24–0.61 and 0.24–0.45, respectively, and the maturity was low mature to mature. Due to the low abundance of N_1S_1, O_1S_1, O_1S_2 and S_2 in crude oil samples, these compounds have changed slightly with maturity. For this study area, the abundance and distribution of compound classes in the crude oil samples did not reflect the strong maturity difference between the sample series.

Fig. 9 shows the relationship between the abundance of DBEs and maturity. It can be seen from the figure that the relative abundance of DBE = 1, 2, 3, 5 is negatively correlated with maturity, while the relative abundance of DBE = 4, 6–17 is positively correlated. That is to say, the abundance of OSCs in high DBEs was positively correlated with maturity, while the OSCs in low DBEs were negatively correlated with maturity. This is because, with the increase of maturity, high DBEs were formed from those with low DBEs through cyclization of alkyl side chains and aromatization [4]. The effect of thermal maturity can be amplified by a selective comparison of the relative abundance of DBE values. DBE_{6-16}/DBE_{1+2+5}-S_1 has a good correlation with thermal maturity (C_{29}-sterane ααα20S/(20S + 20R), C_{29}-sterane αββ/(ααα + αββ)) (Fig. 10a–b). So DBE_{6-16}/DBE_{1+2+5}-S_1 can be used as a maturity parameter.

Figs. 11, S2–S4 show the linear correlation coefficient between maturity and the proportion of S_1 with carbon number ranges of C_{10}-C_{60}, respectively, in the DBE range from10 to 17. It can be seen from Figs. 11, S2 and S3 that maturity is negatively correlated with sulfur compounds with low carbon numbers (C_{10}-C_{34}) and positively correlated with organic sulfur compounds with high carbon numbers (C_{35}-C_{60}). This is due to a series of reactions of violence/thianes to thiophenes to benzo[b] thiophenes to dibenzothiophenes resulting in an increase in carbon numbers in low-mature to mature oils as maturity increases [4]. This study area's maturity of crude oil is relatively low, which explains that maturity is positively correlated with high-carbon organic sulfur compounds. In the higher thermal evolution stage, as maturity increases, thermally induced side-chain cracking leads to the loss of aliphatic hydrocarbons, i.e., reducing sulfur compounds with high carbon numbers in mature to highly mature oils. Nitrogen- and oxygen-containing compounds [31,32] also observed similar phenomena. Further studies are underway to reveal the evolution trend of carbon numbers at high to high maturity levels.

Compared to conventional maturity parameters, the newly developed ratios reported below not only represent the transformation from one compound to another, but also reflect the factors of thermally-induced cyclization, aromatization of hundreds or thousands of compounds. Because C_{10}-C_{14}, C_{15}-C_{19}, C_{20}-C_{24}, C_{25}-C_{29} and C_{30}-C_{34} with DBE = 1–17 are negatively correlated with GC–MS maturity parameters, respectively, and C_{35}-C_{39}, C_{40}-C_{44}, C_{45}-C_{49}, C_{50}-C_{54}, C_{55}-C_{60} with DBE = 1–17 are positively correlated with GC–MS maturity parameters, respectively (Fig. 11; Y-axis is 1–17). Therefore, New maturity parameters include the ratios of compounds with carbon numbers from C_{10}-C_{34} to C_{35}-C_{60} in DBE ranging from 1 to 17. The novel maturity index is defined as C_{35}^{+}/C_{34}-DBE_{1-17}-S_1, showing a very good correlation with Ts/(Ts + Tm) and C_{29}-sterane αββ/(ααα + αββ) (Fig. 10c–d).

Novel thermal maturity and oil-oil correlation parameters by organic

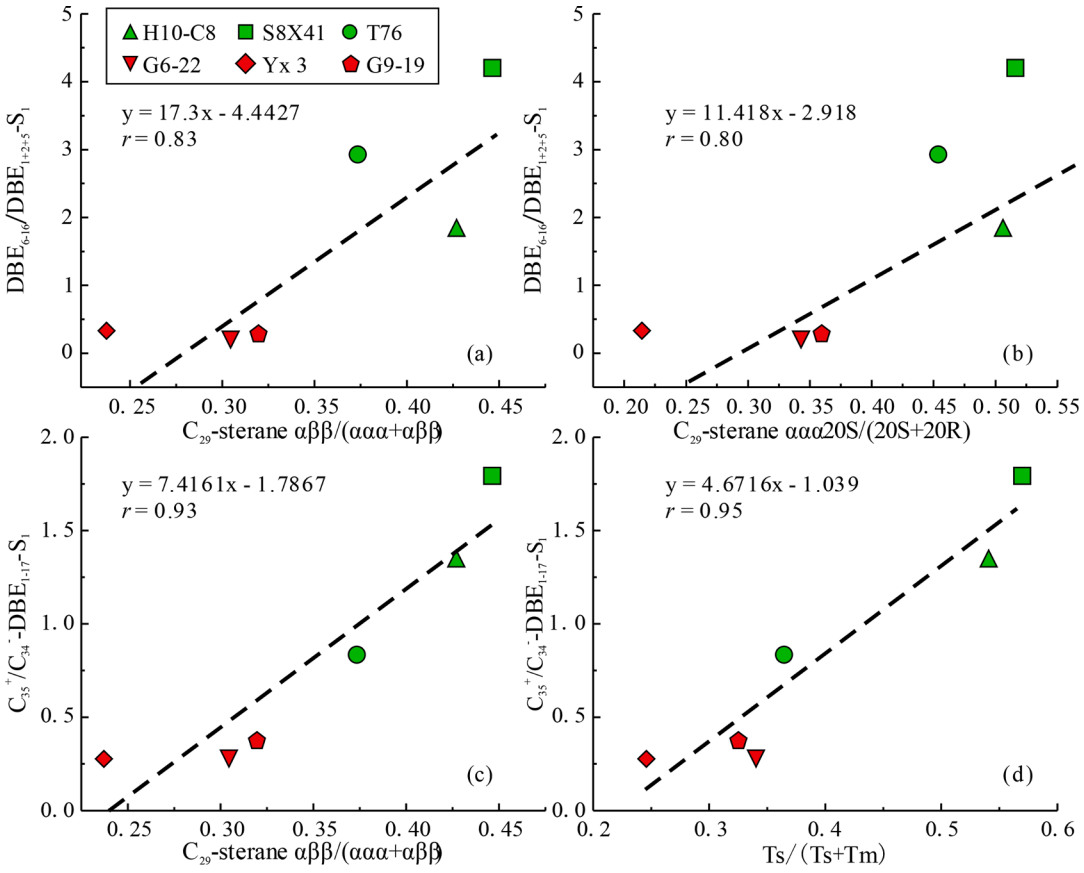

Fig. 10. Cross plots of positive-ion ESI FT-ICR MS indices versus GC–MS parameters for the oils.

sulfur compounds are highly precise and widespread applications in petroleum exploration. We suggest that these development parameters are more suitable for the same type of regions with a low maturity range and need to be slightly adjusted for different regions.

5.3. *Thermochemical sulfate reduction (TSR)*

TSR involves hydrocarbons coupled to the reduction of sulfate in relatively hot (>120∘C) deep carbonate gas reservoirs. In this process, sulfate is reduced to H_2S, resulting in elevated H_2S concentrations (>10 %) [61–65].

Clastic rocks, were well developed in the Dongying Depression, and the oils were shallow buried (1674.8–3461 m) with reservoir maximum temperatures not reaching 120 °C, according to the burial history and well testing data [66–68]. In addition, the Dongying Depression reservoir shows an oil layer or oil–water layer, with no sulfate reduction product H_2S. Thirdly, the $\delta^{34}S$ values of SSNS (G6-22, YX3, G9-19) and CU (H10-C8, S8X41) oils are 19.31 ‰–27.45 ‰ and 16.30 ‰–24.81 ‰ (unpublished data), respectively, showing little variance among isomers (Fig. 12). Since the difference of $\delta^{34}S$ between the SSNS and CU oils and or among the isomers of OSCs in the same crude oil is not obvious, we suggest that TSR alteration in this study is slight or negligible. Further investigation is under the way. Contents of organic sulfur compounds in SSNS and CU oils are significantly different, controlled by sedimentary environment and maturity.

6. Conclusions

The molecular composition of organic sulfur compounds in petroleum samples was selectively characterized through positive-ion ESI FT-ICR MS analysis. S_1 (dominant), O_1S_1, S_2, O_1S_2 and N_1S_1 class species were all detected in low-mature to mature oils deposited under saline and freshwater lacustrine conditions in the Dongying Depression in the Bohai Bay Basin, China. The structure of sulfur compounds is jointly controlled by thermal maturity and hydrocarbon sources. As maturity increases, condensation/aromatization increases, and the number of high-carbon OSCs increases, which are in low-mature to mature oil. Novel parameters based on the relative abundances of the carbon number and DBE ranges (e.g., $DBE_{6–16}/DBE_{1+2+5}$-S_1, C_{35}^{+}/C_{34}-$DBE_{1–17}$-S_1) may be useful as maturity indicators. The OSCs, in most cases, are characterized by their structural resemblance with well-known geologically occurring hydrocarbons and their biochemical precursors, which can be used to study organic input. Other parameters, based on the S-compositions of specific C-numbers, show a relationship with organofacies (e.g., $C_{20}/(C_{19}+C_{21})$-DBE_1-S_1, $C_{40}/(C_{39}+C_{41})$-DBE_3-S_1, $C_{30}/C_{10–55}$-DBE_1-S_1 and $C_{27–29}/C_{10–55}$-DBE_5-S_1), which can be used to provide index values for oil-oil and oil-source correlation.

CRediT authorship contribution statement

Hanjing Zhang: Data curation, Investigation, Writing – original draft. **Sumei Li:** Writing – review & editing, Funding acquisition, Validation.

Declaration of Competing Interest

The authors declare that they have no known competing financial interests or personal relationships that could have appeared to influence the work reported in this paper.

Data availability

Data will be made available on request.

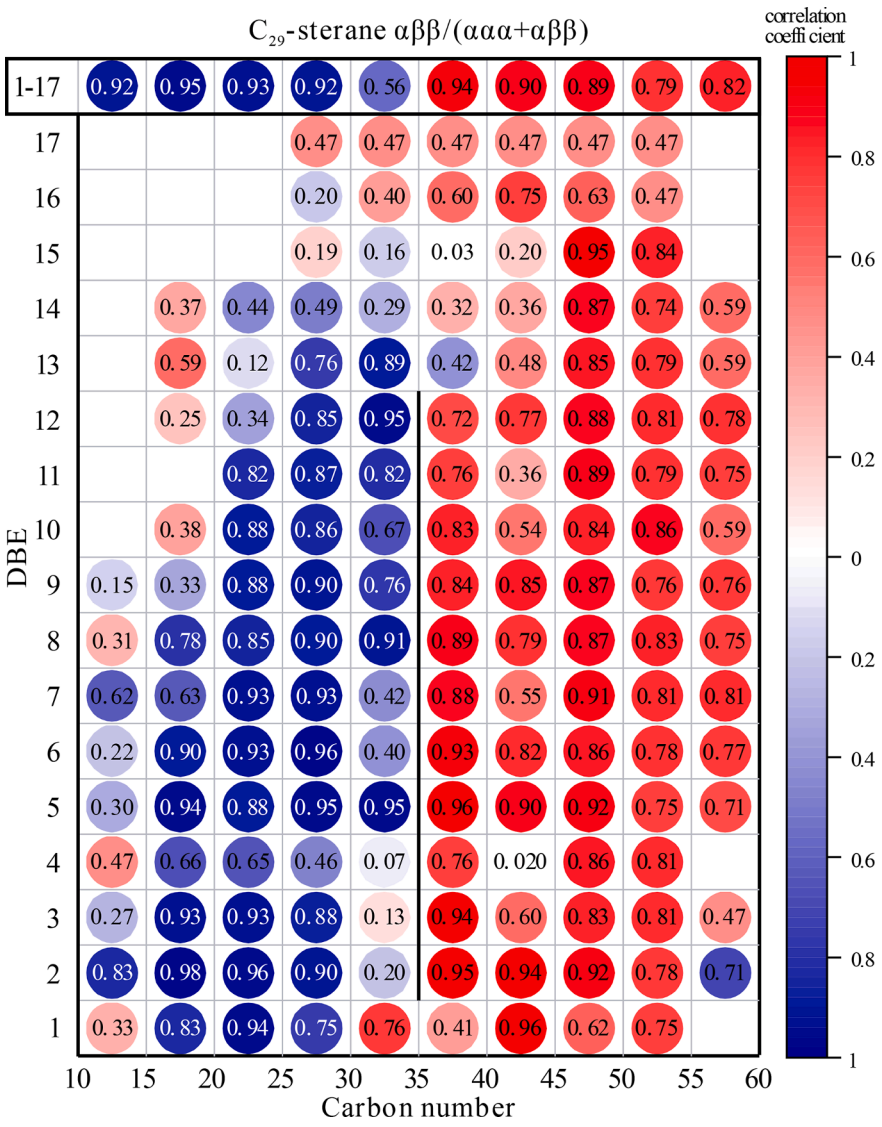

Fig. 11. Percentage content of macromolecular sulfur compounds-to-C_{29}-sterane αββ/(ααα + αββ) comparisons using Pearson's correlation are represented numerically by $|r|$-values and in shades of red (positive correlation) and blue (negative correlation) in SSNS and CU oil. (For example, in Fig. 11, the X-axis is 10–15, and the Y-axis is 1, representing the positive correlation and the correlation coefficient r = 0.33 between the percentage content of sulfur compounds with C_{10-15}-DBE_1 and the maturity parameter of C_{29}-sterane αββ/(ααα + αββ). (For interpretation of the references to color in this figure legend, the reader is referred to the web version of this article.)

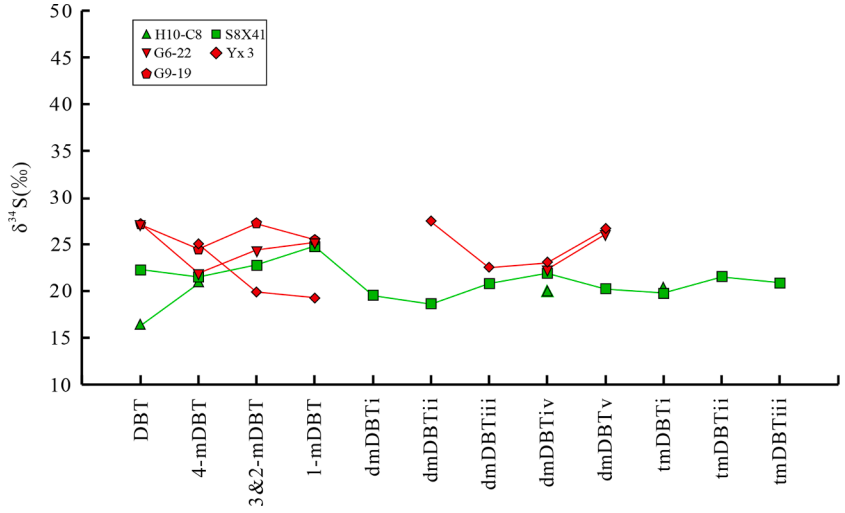

Fig. 12. Distribution pattern of compound specific sulur isotope of the curde oils.

Acknowledgments

This work was supported by the National Natural Science Fundation of China (Grant No. 42073064).

The authors are grateful for the assistance of State Key Laboratory of Heavy Oil of China University of Petroleum for the FT-ICR MS analyses. Several anonymous reviewers are also greatly acknowledged for many helpful and constructive comments on an earlier version of this manuscript.

Appendix A. Supplementary data

Supplementary data to this article can be found online at https://doi.org/10.1016/j.fuel.2022.126408.

References

[1] Orr WL. Sulphur in heavy oils, oils sands and oil shales. In: Strausz OP, Lown EM, editors. In Oil Sand and Oil Shale Chemistry. New York: Verlag Chemie Int; 1978. p. 223–43.
[2] issot BP, Welte DH, Petroleum Formation and Occurrence. (Second Edition). New York: Heidelberg: Springer-Verlag; 1984, p. 699.
[3] Sinninghe Damsté JS, Rijpstra WIC, Kock-van Dalen AC, De Leeuw JW, Schenck PA. Quenching of labile functionalised lipids by inorganic sulphur species: Evidence for the formation of sedimentary organic sulphur compounds at the early stage of diagenesis. Geochim Cosmochim Acta 1989; 53:1343–1355. https://doi.org/10.1016/0016-7037(89)90067-7.
[4] Sinninghe-Damsté JS, Leeuw JW. Analysis structure and geochemical significance of organically-bound sulphur in the geosphere: state of the art and future research. Org Geochem 1990;16(4):1077–101. https://doi.org/10.1016/0146-6380(90)90145-P.
[5] Berner RA, Westrich JT. Bioturbation and the early diagenesis of carbon and sulfur. Am J Sci 1985;285(3):193–206. https://doi.org/10.1016/0198-0254(85)92769-4.
[6] Orr WL, Sinninghe-Damsté JS. Geochemistry of sulphur in petroleum systems. Geochem Sulphur Fossil Fuels Acs Symp 1990;429:2–29. https://doi.org/10.1021/bk-1990-0429.ch001.
[7] Machel HG, Krouse HR, Sassen R. Products and distinguishing criteria of bacterial and thermochemical sulfate reduction. Appl Geochem 1995;10:373–89. https://doi.org/10.1016/0883-2927(95)00008-8.
[8] Sinninghe Damsté JS, Eglinton TI, De Leeuw JW, Schenck PA. Organic sulphur in macromolecular sedimentary organic matter: I. Structure and origin of sulphur-containing moieties in kerogen, asphaltenes and coal as revealed by flash pyrolysis. Geochim Cosmochim Acta 1989;53:873–89. https://doi.org/10.1016/0016-7037(89)90032-X.
[9] Valisolalao J, Perakis N, Chappé B, Albrecht P. A novel sulphur-containing C_{35} hopanoid in sediments. Tetrahedron Lett 1984;25:1183–6. https://doi.org/10.1016/s0040-4039(01)91555-2.
[10] Kohnen MEL, Damsté JSS, Kock-van Dalen AC, Haven HLT, Rullkötter J, De Leeuw JW. Origin and diagenetic transformations of C_{25} and C_{30} highly branched isoprenoid sulphur compounds: further evidence for the formation of organically bound sulphur during early diagenesis. Geochim Cosmochim Acta 1990;54(11):3053–63.
[11] Wakeham S, Sinninghe Damsté JS., Kohnen MEL., De Leeuw JW. Organic sulfur compounds formed during early diagenesis in the Black Sea. Geochim Cosmochim Acta 1995; 59: 521–5. https://doi.org/info:doi/10.1016/0016-7037(94)00361-O.
[12] Wu J, Zhang W, Ma C, Ren L, Li S, Zhang Y, et al. Separation and characterization of squalene and carotenoids derived sulfides in a low mature crude oil. Fuel 2020; 270:117536. https://doi.org/10.1016/j.fuel.2020.117536.
[13] Wu J, Zhang W, Ma C, Wang F, Zhou X, Chung KH, et al. Isolation and characterization of sulfur compounds in a lacustrine crude oil. Fuel 2019;253:1482–9.
[14] Radke M, Welte DH, Willsch H. Maturity parameters based on aromatic hydrocarbons: Influence of the organic matter type. Org Geochem 1986;10(1–3):51–63. https://doi.org/10.1016/0146-6380(86)90008-2.
[15] Li JG. Research development and prospect of maturity parameters of methylated dibenzothiophenes in marine carbonate rocks. Acta Sedimentol Sin 2000;18(3):480–3. https://doi.org/10.14027/j.cnki.cjxb.2000.03.027.
[16] Wei Z, Zhang D, Zhang C, Chen J. Methyldibenzothiophenes distribution index as a tool for maturity assessments of source rocks. Geochim 2001;30(3):242–7. https://doi.org/10.19700/j.0379-1726.2001.03.007.
[17] Orr WL. Changes in sulfur content and isotopic ratios of sulfur during petroleum maturation-study of Big Horn Basin Paleozoic oils. AAPG Bull 1974;58(11):2295–318. https://doi.org/10.1306/83D91B9B-16C7-11D7-8645000102C1865D.
[18] Ho TY, Rogers MA, Drushel HV, Koons CB. Evolution of sulfur compounds in crude oils. AAPG Bull 1974;58:2338–48. https://doi.org/10.1306/83D91BAA-16C7-11D7-8645000102C1865D.
[19] Sun X, Zhang T, Sun Y, Milliken KL, Sun D. Geochemical evidence of organic matter source input and depositional environments in the lower and upper Eagle Ford Formation, south Texas. Org Geochem 2016;98:66–81. https://doi.org/10.1016/j.orggeochem.2016.05.018.
[20] Hartgers WA, Lopez JF, Sinninghe Damsté JS, Reiss C, Maxwell JR, Grimalt JO. Sulfur-binding in recent environments. II. Speciation of sulfur and iron and implications for the occurrence of organo-sulfur compounds. Geochim Cosmochim Acta 1997;61(22):4769–88. https://doi.org/10.1016/S0016-7037(97)00279-2.
[21] Vairavamurthy A, Mopper K. Geochemical formation of organosulphur compounds (thiols) by addition of H_2S to sedimentary organic matter. Nature 1987;329:623–5. https://doi.org/10.1038/329623a0.
[22] Brassell SC, Lewis CA, Leeuw JWD, Lange FD, Damsté JSS. Isoprenoid thiophenes: novel products of sediment diagenesis? Nature 1986;320:160–2. https://doi.org/10.1038/320160a0.
[23] Payzant JD, McIntyre DD, Mojelsky TW, Torres M, Montgomery DS, Strausz OP. The identification of homologous series of thiolanes and thianes possessing a linear carbon framework from petroleums and their interconversion under simulated geological conditions. Org Geochem 1989;14(4):461–73. https://doi.org/10.1016/0146-6380(89)90011-9.
[24] Yang S, Li M, Liu X, Han Q, Wu J, Zhong N. Thermodynamic stability of methyldibenzothiophenes in sedimentary rock extracts: based on molecular simulation and geochemical data. Org Geochem 2019;129:24–41. https://doi.org/10.1016/j.orggeochem.2018.10.012.
[25] Hughey CA, Rodgers RP, Marshall AG, Qian K, Robbins WK. Identification of acidic NSO compounds in crude oils of different geochemical origins by negative ion electrospray Fourier transform ion cyclotron resonance mass spectrometry. Org Geochem 2002;33:743–59. https://doi.org/10.1016/S0146-6380(02)00038-4.
[26] Sinninghe Damsté JS, Leeuw JWD. The origin and fate of isoprenoid C_{20} and C_{15} sulphur compounds in sediments and oils. Int J Environ An Ch 1987;28:1–19. https://doi.org/10.1080/03067318708078398.
[27] Jiang B, Tian Y, Zhai Z, Zhan Z-W, Liao Y, Zou Y-R, et al. Characterisation of heteroatomic compounds in free and bound bitumen from different source rocks by ESI FT-ICR MS. Org Geochem 2021;151:104147.
[28] Peters KE, Walters CC, Moldowan JM. The Biomarker Guide: Biomarkers and Isotopes in Petroleum Systems and Earth History 2005;vol 2:149–490.
[29] Hughey CA, Rodgers RP, Marshall AG, Walters CC, Qian K, Mankiewicz P. Acidic and neutral polar nso compounds in smackover oils of different thermal maturity revealed by electrospray high field fourier transform ion cyclotron resonance mass spectrometry. Org Geochem 2004;35:863–80. https://doi.org/10.1016/j.orggeochem.2004.02.008.
[30] Noah M, Horsfield B, Han S, Wang C. Precise maturity assessment over a broad dynamic range using polycyclic and heterocyclic aromatic compounds. Org Geochem 2020;148:104099. https://doi.org/10.1016/j.orggeochem.2020.104099.
[31] Wan Z, Li S, Pang X, Dong Y, Wang Z, Chen X, et al. Characteristics and geochemical significance of heteroatom compounds in terrestrial oils by negative-ion electrospray Fourier transform ion cyclotron resonance mass spectrometry. Org Geochem 2017;111:34–55.
[32] Ji H, Li S, Greenwoodc P, Zhang H, Pang X, Xue T, et al. Geochemical characteristics and significance of heteroatom compounds in lacustrine oils of the dongpu depression (bohai bay basin, china) by negative-ion fourier transform ion cyclotron resonance mass spectrometry-sciencedirect. Mar Pet Geol 2018;97:568–91. https://doi.org/10.1016/j.marpetgeo.2018.07.035.
[33] Liu W, Liao Y, Shi Q, Samuel Hsu C, Jiang B, Peng P. Origin of polar organic sulfur compounds in immature crude oils revealed by ESI FT–ICR MS. Org Geochem 2018:36–47. https://doi.org/10.1016/j.orggeochem.2018.04.003.
[34] Lu H, Shi Q, Ma Q, Shi Y, Liu J, Sheng G, et al. Molecular characterization of sulfur compounds in some specieal sulfur-rich Chinese crude oils by FT-ICR MS. Science China Earth Sciences 2014;57(6):1158–67. https://doi.org/10.1007/s11430-013-4789-9.
[35] Shi Q, Zhao S, Xu Z, Chung K, Zhang Y, Xu C. Distribution of acids and neutral nitrogen compounds in a chinese crude oil and its fractions: characterized by negative-ion electrospray ionization fourier transform ion cyclotron resonance mass spectrometry. Energy Fuels 2010;24:4005–11. https://doi.org/10.1021/ef1004557.
[36] Han Y, Zhang Y, Xu C, Hsu CS. Molecular characterization of sulfur-containing compounds in petroleum. Fuel 2018;221:144–58. https://doi.org/10.1016/j.fuel.2018.02.110.
[37] Guo X, He S, Liu K, Song G, Wang X, Shi Z. Oil generation as the dominant overpressure mechanism in the cenozoic dongying depression, bohai bay basin. China AAPG Bull 2010;94:1859–81. https://doi.org/10.1306/05191009179.
[38] Cao Y, Yuan G, Li X, Wang Y, Xi K, Wang X, et al. Characteristics and origin of abnormally high porosity zones in buried Paleogene clastic reservoirs in the Shengtuo area, Dongying Sag. East China Pet Sci 2014;11(3):346–62. https://doi.org/10.1007/s12182-014-0349-y.
[39] Zhang Q, Zhu XM, Steel RJ, Zhong DK. Variation and mechanisms of clastic reservoir quality in the Paleogene Shahejie Formation of the dongying sag, bohai Bay Basin. China Petrol Sci 2014;11:200–10. https://doi.org/10.1007/s12182-014-0333-6.
[40] Li S, Pang X, Li M, Jin Z, Qiu Q, Gao Y. Geochemistry of petroleum systems in the Niuzhuang South Slope of Bohai Bay Basin: Part 4. Evidence for new exploration horizons in a maturely explored petroleum province. Org Geochem 2005;36(1135–1150). https://doi.org/10.1016/j.orggeochem.2005.03.004.
[41] Li S, Qiu G, Gao Y, Jiang Z. Formation and Accumulation of Hydrocarbons in the Central Uplift, Dongying Depression. Petrol Sci 2006; 3:12–22. https://doi.org/NKI:SUN:SYKX.0.2006-03-001.
[42] Guo X, Liu K, Sheng H, Song G, Wang Y, Hao X, et al. Petroleum generation and charge history of the northern Dongying Depression, bohai bay basin, china: insight from integrated fluid inclusion analysis and basin modelling. Mar Pet Geol 2012;32(1):21–35. https://doi.org/10.1016/j.marpetgeo.2011.12.007.

[43] Chang CY. Geological characteristics and distribution patterns of hydrocarbon deposits in the bohai bay basin, east china. Mar Pet Geol 1991; 8:98–106. https://doi.org/10.1016/0264-8172(91)90048-6.
[44] Pang X, Li M, Li S, Jin Z. Geochemistry of petroleum systems in the Niuzhuang South Slope of Bohai Bay Basin. Part 3: estimating hydrocarbon expulsion from the shahejie formation. Org Geochem 2005;36(4):497–510. https://doi.org/10.1016/j.orggeochem.2004.12.001.
[45] Li S, Pang X, Jin Z, Li M, Liu K, Jiang Z, et al. Molecular and isotopic evidence for mixed-source oils in subtle petroleum traps of the Dongying South Slope. Bohai Bay Basin Mar Pet Geol 2010;27(7):1411–23. https://doi.org/10.1016/j.marpetgeo.2010.04.004.
[46] Zhang L, Zhang C. The mechanism and system for low mature crude oil formation: the case study of oils in Niuzhuang Depression, Jiyang Basin [M]. Beijing: Geological Publishing House; 1999. p. 120–1.
[47] Wang M, Zhao S, Chung KH, Xu C, Shi Q. Approach for selective separation of thiophenic and sulfidic sulfur compounds from petroleum by methylation/demethylation. Anal Chem 2015;87(2):1083–8.
[48] Emerson RW. Causation and pearson's correlation coefficient. J Visual Impairm Blindness 2015;109(3):242–4. https://doi.org/10.1177/0145482X1510900311.
[49] Makou M, Eglinton T, Mcintyre C, Montluon D, Antheaume I, Grossi V. Plant wax n -alkane and n -alkanoic acid signatures overprinted by microbial contributions and old carbon in meromictic lake sediments. Geophys Res Lett 2018;45:19–20. https://doi.org/10.1002/2017GL076211.
[50] Gelpi E, Schneider H, Mann J, Oró J. Hydrocarbons of geochemical significance in microscopic algae. Phytochemistry 1970; 9: 603–612. https://doi.org/10.1016/S0031-9422(00)85700-3.
[51] Connan J, Cassou AM. Properties of gases and petroleum liquids derived from terrestrial kerogen at various maturation levels. Geochim Cosmochim Acta 1980; 44:1–23. https://doi.org/10.1016/0016-7037(80)90173-8.
[52] Sinninghe Damsté JS, Kenig F, Koopmans MP, Koster J, Schouten S, Hayes JM, et al. Evidence for gammacerane as an indicator of water column stratification. Geochim Cosmochim Acta 1995;59:1895–990. https://doi.org/10.1016/0016-7037(95)00073-9.
[53] Moldowan JM, Seifert WK, Gallegos EJ. Identification of an extended series of tricyclic terpanes in petroleum. Geochim Cosmochim Acta 1983;47:1531–4. https://doi.org/10.1016/0016-7037(83)90313-7.
[54] Haven HLT, Leeuw JWD, Peakman TM, Maxwell JR. Anomalies in steroid and hopanoid maturity indices. Geochim Cosmochim Acta 1986;50(5):853–5.
[55] Kvalheim OM, Christy AA, Telnaes N, Bjørseth A. Maturity determination of organic matter in coals using the methylphenanthrene distribution. Geochim Cosmochim Acta 1987;51:1883–8. https://doi.org/10.1016/0016-7037(87)90179-7.
[56] Radke M, Welte DH, Willsch H. Geochemical study on a well in the western canada basin: relation of the aromatic distribution pattern to maturity of organic matter. Geochim Cosmochim Acta 1982;46(1):1–10.
[57] Peters KE, Coutrot D, Nouvelle X, Ramos LS, Rohrback BG, Magoon LB, et al. Chemometric differentiation of crude oil families in the San Joaquin Basin. California AAPG Bull 2013;97:103–43. https://doi.org/10.1306/05231212018.
[58] Urban NR, Ernst K, Bernasconi S. Addition of sulfur to organic matter during early diagenesis of lake sediments. Geochim Cosmochim Acta 1999;63:837–53. https://doi.org/10.1016/S0016-7037(98)00306-8.
[59] Filley TR, Freeman KH, Wilkin RT, Hatcher PG. Biogeochemical controls on reaction of sedimentary organic matter and aqueous sulfides in Holocene sediments of Mud Lake. Florida Geochim Cosmochim Acta 2002;66:937–54. https://doi.org/10.1016/S0016-7037(01)00829-8.
[60] Volkman JK. A review of sterol markers for marine and terrigenous organic matter. Org Geochem 1986;9:84–99. https://doi.org/10.1016/0146-6380(86)90089-6.
[61] Cai C, Worden RH, Bottrell SH, Wang L, Yang C. Thermochemical sulphate reduction and the generation of hydrogen sulphide and thiols (mercaptans) in Triassic carbonate reservoirs from the Sichuan Basin. China Chem Geol 2003;202(1–2):39–57. https://doi.org/10.1016/S0009-2541(03)00209-2.
[62] Cai C, Zhang C, Cai L, Wu G, Jiang L, Xu Z, et al. Origins of Palaeozoic oils in the Tarim Basin: Evidence from sulfur isotopes and biomarkers. Chem Geol 2009;268(3-4):197–210.
[63] Cai C, Amrani A, Worden RH, Xiao Q, Wang T, Gvirtzman Z, et al. Sulfur isotopic compositions of individual organosulfur compounds and their genetic links in the Lower Paleozoic petroleum pools of the Tarim Basin. NW China Geochim Cosmochim Acta 2016;182:88–108.
[64] Amrani A, Deev A, Sessions AL, Tang Y, Adkins JF, Hill RJ, et al. The sulfur-isotopic compositions of benzothiophenes and dibenzothiophenes as a proxy for thermochemical sulfate reduction. Geochim Cosmochim Acta 2012;84:152–64.
[65] Walters CC, Wang FC, Qian K, Wu C, Mennito AS, Wei Z. Petroleum alteration by thermochemical sulfate reduction–A comprehensive molecular study of aromatic hydrocarbons and polar compounds. Geochim Cosmochim Acta 2015;153:37–71. https://doi.org/10.1016/j.gca.2014.11.021.
[66] Luan G, Dong C, Azmy K, Lin C, Ma C, Ren L, et al. Origin of bedding-parallel fibrous calcite veins in lacustrine black shale: a case study from Dongying Depression, Bohai Bay Basin. Mar and Petrol Geol 2019;102:873–85. https://doi.org/10.1016/j.marpetgeo.2019.01.010.
[67] Qiao R, Chen Z, Li C, Wang D, Gao Y, Zhao L, et al. Geochemistry and accumulation of petroleum in deep lacustrine reservoirs: a case study of Dongying Depression, Bohai Bay Basin. J Petrol Sci Eng 2022;213:110433.
[68] Ping H, Chen H, Jia G. Petroleum accumulation in the deeply buried reservoirs in the northern Dongying Depression, Bohai Bay Basin, China: New insights from fluid inclusions, natural gas geochemistry, and 1-D basin modeling. Mar and Petrol Geol 2017;80:70–93. https://doi.org/10.1016/j.marpetgeo.2016.11.023.